

Insight into heterogeneous karst catchment by the dynamical system approach

Simon Rusjan^{*}, Klauđija Lebar, Nejc Bezak

University of Ljubljana, Faculty of Civil and Geodetic Engineering, Chair of Hydrology and Hydraulic Engineering, Jamova 2, SI-1000 Ljubljana, Slovenia

ARTICLE INFO

Keywords:

Karst springs
Karst sinking streams
Discharge recession
Sensitivity function
Dynamic karst catchment storage

ABSTRACT

The hydrological process heterogeneity in karst catchments makes collecting sufficient information about the karst system properties extremely difficult. Consequently, the parameterization and application of currently available modeling approaches is highly uncertain in karst. We implemented a modified dynamical system approach and explored the possibilities to analyze, simulate and characterize karst springs and sinking streams in the heterogeneous Ljubljana river catchment in Slovenia. The discharge sensitivity functions were used to simulate the hydrographs and identify the differences in the temporal dynamics of the discharge recession. Most of the derived karst springs and sinking streams discharge sensitivity functions express dual discharge recession behavior most likely controlled by the hydraulic conveyance characteristics of karst underground conduits. The implemented approach offers a high potential for advancement in karst hydrology by using basic discharge data for analyses of karst catchment characteristics and future planning of karst water resource management.

1. Introduction

Karst aquifers are a drinking water reservoir for roughly 20–25% of the global population (Ford and Williams, 2007; Hartmann et al., 2017). Climate simulations project a strong increase in air temperature and a decrease of precipitation in many karst regions in the world over the next decades, which will undoubtedly influence the water availability in karst aquifers (Hartmann et al., 2014; Liu et al., 2018). The hydrological behavior of a karst system can be characterised by temporally and spatially highly variable processes of recharge (diffuse and concentrated), storage (in epikarst, vadose, and phreatic zones), and flow formation (diffuse and along preferential conduits) (White, 2002). Consequently, karst catchments as hydrological systems express a high degree of aquifer structure heterogeneity as a result of interacting processes of concentrated and diffuse infiltration, varying flow formation along the underground conduit systems that can extend over long distances (Ravbar et al., 2012; Zhang et al., 2022). While the hydrological characteristics of many karst systems are conceptually relatively well described, the contribution of particular runoff formation processes during contrasting hydrological conditions is usually difficult to quantify.

Springs have been recognized as one of the most important hydrogeological features of karst catchments, since karst underground systems

are able to concentrate discharge from wide catchment areas in a single point (Hartmann et al., 2014). The physical characteristic of karst springs (discharge, water physical and chemical characteristics) can be relatively easily monitored and provide fundamental knowledge on karst aquifer storage characteristics. The main hydraulic characteristic of karst aquifers is their heterogeneity; their storage consists of complex conduit networks, which are “immersed” in a low-permeability fractured limestone volume (Király, 2002). Intermittent karst springs dry up during long dry periods but can exhibit a large increase in discharges following intense precipitation (Kresic and Stevanovic, 2009). At karst springs, discharge variations by factors of 10 to 100 within hours or days are common, water tables in caves and karst aquifers can vary by several tens of meters or more (Bonacci and Roje-Bonacci, 2000).

Systematic records of karst spring discharges allow for the definition of the hydrological regime, while hydrograph formation analyses provide a useful tool to evaluate karst aquifer storage characteristics (Bonacci, 1993; White, 2007; Schmidt et al., 2014). It is believed that hydrogeological, geometrical and hydraulic characteristics of a karst aquifer storage can be distinguished by the hydrograph recession dynamics (Fiorillo, 2014). These facts have stimulated numerous studies, trying to develop the analytical expressions that would relate the discharge recession dynamics to the karst storage physical characteristics. Systematic reviews of hydrograph recession analyses specific for the

^{*} Corresponding author.

E-mail address: simon.rusjan@fgg.uni-lj.si (S. Rusjan).

karst environment can be found in Ghasemizadeh et al. (2012) and Fiorillo (2014). There were attempts to implement empirical (e.g. Dewandel et al., 2003), conceptual (e.g. Mazzilli et al., 2012) or physically-based (e.g. Kresic, 2007) models which tried to relate the recession behavior of karst springs to some pre-defined geometric and hydraulic characteristics of the karst storage by introducing different equation parameters. In practical terms of data availability, the study of the karst catchment storage behavior is usually conditioned by the position of the water stations where discharge is measured. However, one of the main problems of abovementioned modeling approaches remains the difficulty of relating the models' parameters to physical characteristics of the karst catchment storage. Karst catchments represent complex hydrological systems, difficult to be presented well with pre-defined conceptual models (Bonacci and Andrić, 2015). The spatial heterogeneity and process complexity of karst subsurface flow imply that any feasible hydrological model will necessarily involve substantial simplifications and generalization. Further conceptualization of streamflow generation processes in karst and their integration into rainfall-runoff models remains one of the major research challenges in karst catchment hydrology (White, 2002).

The reason that most existing models are able to consider only some, but not all important karst processes and karst storage characteristics, is the need for inclusion of many model parameters, which often could not be linked to physically meaningful or measurable landscape properties (Atkinson et al., 2002; Kavetski et al., 2011). Further this may lead to model over-parametrization. Kirchner (2009) demonstrated how streamflow time series can be used to acquire a storage-discharge relationship that can be applied to simulate a full range of streamflow conditions when combined with precipitation and evapotranspiration data. The model structure was conceptualized on the system properties, which were directly inferred from observed changes during streamflow recession. Other recent researches (e.g. Shaw and Riha, 2012; Brauer et al., 2013; Adamovic et al., 2015; Birkel et al., 2015; Rusjan and Mikoš,

2015; Staudinger et al., 2017; Maneta et al., 2018) in various hydrogeological settings have increased confidence that streamflow recession does not necessarily solely reflect aquifer characteristics but instead provides a broader measure of the system-wide storage-discharge and even hydrogeological characteristics within catchments. In view of karst catchments, the storage-discharge relationship derived directly from observed karst spring discharges could provide valuable information on the changing nature of underground flow and karst storage characteristics, which can change abruptly along the preferential underground flow paths or under changing hydrological conditions. The application of the theory is challenging especially in catchments with heterogeneous hydrogeology.

In this study we implemented a modified dynamical system approach to describe the hydrological responses of different parts of a complex karst hydrological system of the Ljubljana river in Slovenia. Highly hydrologically heterogeneous karst springs fed by deep underground flows and karst intermittent streams which collect water mainly from local surface and near-surface flows were included in the analysis to distinguish differences in their karst storage characteristics. The goals of the study were to: (1) Use long-term daily data on karst spring flows to obtain insight into the storage-discharge relationships by estimating the sensitivity of discharge to changes in a catchment storage; (2) Implement the modified dynamical system approach for karst springs and sinking streams discharge simulations in contrasting seasonal hydrological conditions; (3) Improve our understanding of the karst storage characteristics in different hydrological conditions and compare the results with previous hydrological studies of the study area.

2. Study catchment and data availability

The Ljubljana river catchment (approx. 1880 km²) belongs to the classical karst area in Slovenia (Fig. 1). Generally, the catchment can be characterised as a hydrologically highly heterogeneous karst area with

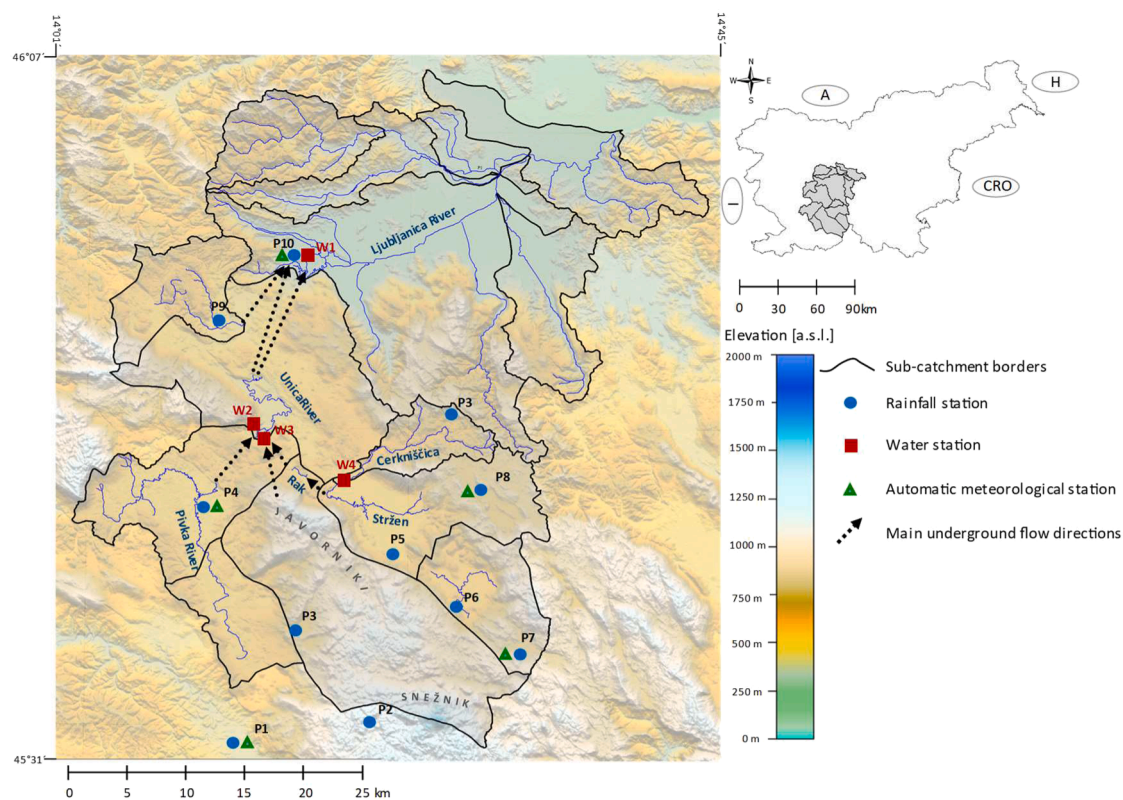


Fig. 1. The Ljubljana river catchment. Dashed arrows illustrate the main underground flow directions. Sub-catchment borders were defined by combined topography and tracer data analysis made in the past.

variable terrain topography (altitudes ranging from 300 m a.s.l. to 1800 m a.s.l.). The terrain topography strongly influences the rainfall spatial distribution over the catchment. The highest rainfall sums are measured along the orographic barriers of the Snežnik karst plateau (rainfall sums above 3000 mm/year) and along the Javorniki karst plateau (rainfall sums exceeding 2000 mm/year). The long-term mean annual rainfall in the north-eastern part of the Ljubljana river catchment is approx. 1400 mm/year and the mean air temperature ranges between 8 and 10 °C. The long-term mean annual reference evapotranspiration (dataset period 1961–2016, Penman-Monteith equation) at station P4 is 720 mm. The long-term mean annual evapotranspiration at the highest meteorological station P7 (760 m a.s.l.) and at the lowest-lying meteorological station P10 (293 m a.s.l.) is 660 mm and 780 mm, respectively. The mean monthly reference evapotranspiration at meteorological station P4 for the winter months (December – February) is 15 mm and increases to 112 mm for the summer months (June – August).

In terms of hydrogeological characteristics, the karst part of the catchment consists of fissured, highly porous carbonate rock (mainly limestone and dolomite); non-carbonate rocks prevail only in the northern, lowland part of the catchment. The complex hydrogeological structure of the karst hinterland area strongly affects the surface river network, causing rivers and streams to sink underground several times along the main flow directions. The hydrogeological characteristics of the Ljubljana river catchment have been investigated by several studies (e.g., Gams, 1970; Gospodarič and Habič, 1976; Blatnik et al., 2017); the main findings are summarized below.

In the headwater, heavily karstified part of the Ljubljana river catchment, the main river is the Unica and its tributary, the Malenščica river. The Unica river catchment consists of three hydrologically interconnected parts, i.e. the Javorniki, Pivka, and Cerknica. The central area (Javorniki part) consists of Javorniki and Snežnik karst massifs. Eastwards, the Javorniki part borders the Pivka river valley; at the western side, a series of karst poljes can be found (the Cerknica polje being the largest). The Javorniki karst plateau is composed of well-karstified Jurassic and Cretaceous limestones with karst-fissure porosity (Ravbar et al., 2012). In this part of the catchment, underground flow dominates, while several surface streams can be found in the other two parts. Poorly permeable Eocene flysch covers the Pivka river valley and enables the development of the surface network of the Pivka river. The Pivka river sinks into the Postojna Cave and reappears at the surface as the Unica spring (Petrič, 2010). Most of the smaller karst streams have an intermittent character as they are recharged mainly by rainfall runoff from karst; after appearing as surface flows, they sink underground again. Further downstream, the Unica river sinks along the northern edge of the Planinsko polje and re-appears as the Ljubljana river at several springs aligned along the south-western border of the Ljubljana Marshes. The long-term mean daily discharge calculated from the available daily discharge dataset at water station W1 is 24 m³/s, while the mean daily discharges can go down to approx. 1 m³/s during longer rainless periods. The meteorological and hydrological monitoring system is shown in Fig. 1. Karst springs and sinking streams data are summarized in Table 1. For water stations W1 and W2, long-term daily discharge data date back to 1926, while hourly discharge data have been available since 1998 for water stations W1 and W4. At water station W3, the hourly discharge data are available from late 2016. The spatial extension of the complex karst underground conduit system of the Ljubljana river is strongly conditioned by the hydrological conditions, making the delineation of effective catchment areas very difficult. The catchment areas data in Table 1 were assessed from various tracer test applications combined by the topography analysis in some parts of the catchment.

In more recent hydrogeological studies (e.g., Kogovšek and Petrič, 2010; Gabrovšek et al., 2010; Ravbar et al., 2012; Kogovšek and Petrič, 2014; Petrič et al., 2018; Rusjan et al., 2019), various natural and artificial tracers were used to improve the understanding of the extremely complex karst underground flow formation, which varies considerably

Table 1
Karst springs and sinking streams water station data summary.

Location	Name	Type	Catchment area [km ²]	Mean/Max./Min. discharge [m ³ /s]	Data period
W1	Vrhnika	spring	~1100	24.1/121.2/1.0	1926- (daily); 1998- (hourly)
W2	Unica	sinking river	~840	22.2/90.2/0.9	1926- (daily); 2005- (hourly)
W3	Malenščica	spring	~750	6.7/11.2/1.1	1961- (daily); 2016- (hourly)
W4	Cerkniščica	sinking stream	58	1.1/37.3/~0	1961- (daily); 1998- (hourly)

both spatially and temporally. There have also been efforts to apply a rainfall-runoff model to simulate the daily discharge dynamics at a few karst springs and water stations in the karst part of the Ljubljana catchment using a lumped conceptual and data mining model (Sezen et al., 2018, 2019). However, the main problem of similar hydrological modeling attempts remains how to relate the pre-defined hydrological model concepts to the characteristics of a complex heterogeneous karst catchment that could be identified through discharge recession dynamics, chemical and physical parameters monitoring, and tracer test applications.

3. Methods

3.1. Estimation of sensitivity functions

In karst catchments, the discharge in the karst springs and sinking streams is controlled by the characteristics of the karst underground storage. There have been several attempts to relate the observed temporal discharge dynamics to characteristics of underground karst storage systems. Kirchner (2009) proposed a relatively straightforward method for determining the non-linear storage (reservoir) parameters for a simple bucket model with the assumption that discharge Q depends uniquely on total water storage S in the catchment. This sounds appealing especially for describing underground storage-controlled catchments, such as karst catchments. However, according to our knowledge, there were no attempts to explore the general applicability of the dynamical system approach in typical karst catchments, such as the Ljubljana river catchment. The catchment dynamical system characterization is based on water balance equation where the total catchment storage variation is estimated using:

$$\frac{dS}{dt} = P - ET - Q \quad (1)$$

Where S is the volume of water stored in the catchment (in units of depth – mm of water). P , ET , and Q are rates of precipitation, actual evapotranspiration, and discharge (all in mm of water), respectively. All variables in Eq. (1) are understood to be functions of time and spatially averaged over whole catchment area. The precipitation and evapotranspiration rates can be highly spatially variable and are usually obtained by point measurements. In the Ljubljana river catchment, the detailed information on precipitation and evapotranspiration spatial variability is difficult to acquire due to the versatile topography and complex seasonal precipitation formation patterns (Krklec et al., 2018). This makes the spatial extrapolation of precipitation and evapotranspiration estimates extremely difficult. Since the main stress in the study

was not on the use of complex spatial data interpolation techniques, the spatial variability in precipitation data was considered by the Thiessen polygons. The reference evapotranspiration estimates were based on the Penman-Monteith method. The main assumption in the spatial extrapolation of the reference evapotranspiration estimates was that the air temperature decrease with increasing altitude plays the most important role. Therefore, we analyzed the altitude effect between the meteorological stations where data on the reference evapotranspiration were available. Based on the calculated average terrain altitude, the average reference evapotranspiration was assessed for each meteorological station's Thiessen polygon.

Stream discharge as an environmental flux could be considered as a quasi-state variable that characterizes the entire catchment in Eq. (1). Kirchner (2009) suggested that there is a catchment characteristic function $f(S)$ that relates the discharge at catchment outlet Q to the total storage in catchment S :

$$Q = f(S) \text{ or } S = f^{-1}(Q) \quad (2)$$

In view of the rainfall runoff formation, karst springs could be a good example of such a relation. Differentiating eq. (2) with respect to time and substituting Eq. (1), eq. (3) can be obtained:

$$\frac{dQ}{dt} = \frac{dQ}{dS} \frac{dS}{dt} = \frac{dQ}{dS} (P - ET - Q) \quad (3)$$

Kirchner (2009) used the derivative of $f(S)$ rather than $f(S)$ directly in order to overcome some of the practical limitations of estimating catchment storage S :

$$\frac{dQ}{dS} = f'(S) = f'(f^{-1}(Q)) = g(Q) \quad (4)$$

In eq. (4) $g(Q)$ is named the ‘‘sensitivity function’’. In our study it expresses the karst spring/sinking stream discharge sensitivity to changes in the karst catchment storage. By combining eq. (3) and eq. (4), $g(Q)$ can be expressed as:

$$g(Q) = \frac{dQ}{dS} = \frac{dQ/dt}{dS/dt} = \frac{dQ/dt}{P - ET - Q} \quad (5)$$

The sensitivity function represents the aggregated response of specific karst spring/sinking stream draining specific parts of the analyzed karst catchment. One should not expect that the discharge sensitivity function is able to agree all different karst storage units in unsaturated and saturated parts of the karst matrix, which can be extremely heterogeneous in terms of its hydraulic properties or storage characteristics and can change abruptly during different hydrological conditions.

In order to avoid problems with P and ET data availability over whole catchments, Kirchner (2009) suggested assessing the sensitivity functions from the periods when P and ET are relatively small compared to discharge, e.g. rainless night periods. In our approach, the sensitivity functions are derived from long-term (> 50 years) daily discharge records. There are two practical reasons for using daily discharges instead of hourly discharges: (1) The available daily discharge datasets are generally much longer whereas, as in our case, the hourly discharges on many stations are available only for the last few years. (2) Discharge recession on many of the karst springs/sinking streams can be very slow; consequently, there is often no ‘‘detectable’’ change in the discharge between the consecutive hourly records making the analysis of hourly discharge recession rates difficult. This is especially problematic during low-flow conditions. Therefore, for estimating $g(Q)$ we used daily discharges recession data from the arbitrarily defined periods when the daily precipitation sum for the preceding two days was less than 2 mm over the karst spring/sinking stream sub-catchment. To further limit the possible influence of ET on the karst springs' discharge recession, the discharge recession records from dormant periods (November to February) were accounted. Fig. 2 shows seasonal variability in long-term mean daily reference ET at station P4 (for the period 1961–2016). During the November–February period, the mean daily reference

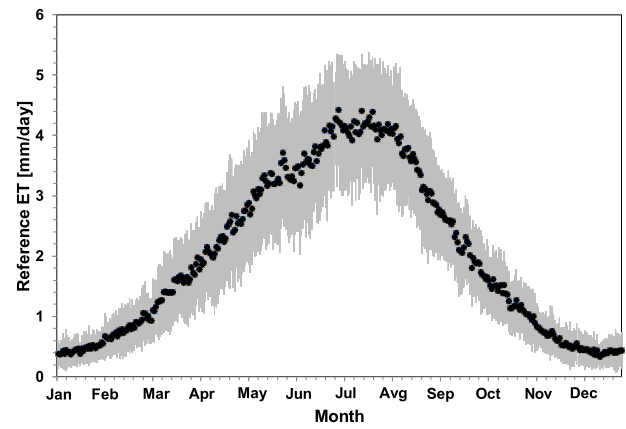


Fig. 2. Seasonal variability in long-term daily reference evapotranspiration at station P4. The black dots and gray lines indicate the means and standard deviations, respectively.

evapotranspiration is generally well below 1 mm/day. A similar seasonal ET pattern could be observed at other meteorological stations in the catchment.

Data from the selected rainless late autumn and winter discharge recession periods were further used to construct the recession plots of the flow recession rate ($-dQ/dt$). The flow recession rate was estimated as a difference between two successive days and the discharge was averaged over those two days. Binning was then done by grouping the individual daily data into ranges of Q and then calculating the standard and mean error for $-dQ/dt$ and Q for each bin. The mean hourly change in discharge was calculated by dividing the mean daily change in discharge by 24 h. One or two quadratic curves (depending on the form of the storage-discharge relationship) were fitted to the binned means by the least-square regression with inverse variance weighting, leading to the following empirical equation in log space:

$$\ln(g(Q)) = \ln\left(-\frac{dQ/dt}{Q} \middle| P \ll Q, ET \ll Q\right) \approx x_1 + x_2 \ln(Q) + x_3 (\ln(Q))^2 \quad (6)$$

where x_1 , x_2 , and x_3 are parameters of the fitted quadratic curves. The quadratic curves in a general form given in eq. (6) were used to incorporate the characteristics of sensitivity functions $g(Q)$ in hydrograph simulations.

3.2. Hydrograph simulation

The derived sensitivity functions were further used to perform hydrograph simulations for the selected karst springs and sinking streams. Using eq. (5) and replacing dS/dt in eq. (3) with water balance eq. (1), we obtained differential eq. (7) to describe changes in the discharge where quadratic function of eq. (6) is used to describe $g(Q)$,

$$\frac{dQ}{dt} = \frac{dQ}{dS} \frac{dS}{dt} = g(Q)(P - r - k_{ET} \cdot ET - Q) \quad (7)$$

To estimate the ET term in eq. (7) we used the Penman-Monteith reference evapotranspiration available for several meteorological stations in the area (Fig. 1). For the period 1961–2015, only daily reference ET values are available. After 2015, hourly meteorological data needed for calculating hourly reference evapotranspiration used for hydrograph simulations are available on most of the meteorological stations in the catchment. For other years, the hourly ET values at the meteorological stations were approximated by multiplying the calculated daily ET values with the seasonal ‘‘weighting factors’’ shown in Fig. 3(a). The factors present the normalized mean hourly distribution of ET values during a day in different seasons. The mean hourly distribution of ET values was derived by accounting the hourly meteorological data in the

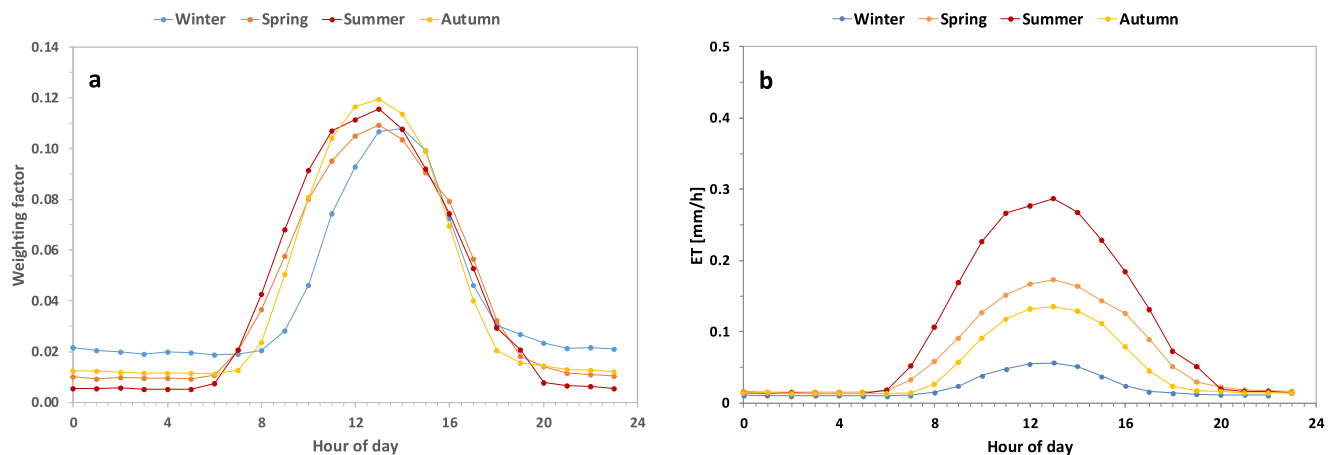


Fig. 3. (a) Normalized mean hourly distribution of ET values during a day in different seasons. (b) Mean hourly distribution of reference ET values during a day in different seasons.

Penman-Monteith equation at meteorological station P4 during period 2015–2016. For a comparison, the mean hourly distributions of ET values during various seasons are shown in Fig. 3(b). Although there could be a considerable variability in the hourly distribution of ET values during a particular day, one should have in mind that the variance in ET values is much smaller than that in precipitation or discharge. Consequently, the potential impact of hourly ET values temporal distribution is in our view relatively limited.

In eq. (7) r and k_{ET} are the mass conservation ratio and the evapotranspiration scaling parameter, respectively. Numerous attempts can be found in literature to fit the calculated reference ET in different hydrological modeling applications (e.g. Abbaspour et al., 2007; Efstratiadis and Koutsoyiannis, 2010). In order to account for the differences between the actual and reference evapotranspiration, an evapotranspiration scaling coefficient k_{ET} was used as a calibration parameter for the hydrograph simulations. The evapotranspiration scaling coefficient are usually strongly vegetation type and seasonally dependent McMahan et al., 2013). In our approach, single value of k_{ET} was defined based on multiple simulation runs. For the possible consideration of an additional “unknown” rainfall loss not covered by the $K_{ET} \cdot ET$ product in eq. (7), a ratio “ $r = (Q + k_{ET} \cdot ET) / P$ ” between the output of the catchment as the sum of the discharge and reference evapotranspiration vs. the input into the catchment (sums of rainfall) was introduced to close the mass balance. The corresponding r parameter value was defined by considering catchment water mass balance (sums of Q , ET and P in mm) for the selected 1-year simulation periods between 2012 and 2017. In karst catchments, inconsistency in mass balance could be related to uncertainties in (1) the time variant spatial extension of the karst catchment areas Hartmann et al., 2013) and (2) the temporal dynamics of water fluxes and storages in karst conduits and fissures which may become hydrologically disconnected Rusjan et al., 2019). The above-mentioned processes may vary considerably during changing hydrological conditions (Bonacci, 2004; Ravbar et al., 2011; Chen et al., 2018). Finally, to assess how the simulation results fit the observations, we used: (1) the Nash-Sutcliffe efficiency (NSE) criteria; (2) Nash-Sutcliffe efficiency criteria with logarithmic values (NSE_{ln}) in order to increase the sensitivity of the NSE efficiency criteria to systematic model over- or underprediction, especially the sensitivity to the influence of the low-flow values.

In solving eq. (7), attention should be paid to two details, i.e. time lags and potential numerical instabilities. The changes in subsurface storage lag behind the rainfall inputs due to the delays necessary for rainfall to infiltrate and influence the discharge at the outlet (e.g. karst spring). Time lags could be extremely diverse in hydrologically heterogeneous catchments such as karst catchments where epikarst porosities, percolation through the vadose zone and along the underground

conduits can vary greatly over small spatial scales. Consequently, at the Ljubljana river study catchment, we were unable to distinguish the lag-time for selected karst springs/sinking streams from input precipitation data and include them directly into the hydrograph simulations. We assessed the lag-time by performing post-simulation cross-correlation analysis between measured and modelled discharges using the time steps of 1 to 24 h. The lag-time that showed the best correlation was considered in the simulation performance assessment. Eq. (7) was solved numerically on an hourly time step using its log-transform to minimize numerical instabilities by applying the fourth-order Runge-Kutta integration. A single value of measured discharge was used to initialize simulation for the 1-year periods.

4. Results

4.1. Sensitivity functions of the karst springs and sinking streams

From the recession plots of daily discharge data for the period 1961–2016 shown in Fig. 4 on a log scale, a significant scatter in the recession rates is evident. From the process point of view, the recession rate scatter could be related to changing karst storage emptying dynamics related to specific hydrological conditions. An additional factor could be the presence of snow as discussed by Teuling et al. (2010). Snow cover can persist in the area of the Snežnik plateau and the Javorniki ridge during longer winter periods. Snowmelt can occur gradually during seasonal temperature transitions; however, the snow often melts abruptly due to quick temperature rises in combination with abundant rainfall events. Such a hydro-meteorological situation is fairly common in late fall, winter or early spring and is the most problematic in terms of floods. On the other hand, some of the data scatter could also arise from random measurement noise or errors and coarse graining due to finite discretization of discharge measurements, and thus of calculated flow recession rates (visually evident from the presence of horizontal stripes in Fig. 4). Binned mean discharges with the highest recession rates at stations W1 and W2 are rather similar (binned mean discharge of 0.14 mm/h or 42 m³/s at station W1 and 0.20 mm/h or 47 m³/s at station W2). This might indicate a common discharge recession mechanism at both stations controlled by the hydraulic conveyance of the karst underground conduits system separating the two stations. Station W2 is positioned upstream, before the Unica river sinks underground, and station W1 downstream where the river comes back to the surface as the Ljubljana river.

Fig. 5 shows the binned mean hourly recession rates and the fitted quadratic functions (curves) which express the sensitivity functions $g(Q)$ in log values. The binned means (black and gray dots) generally deviate from the fitted regression lines by less than their standard errors. The

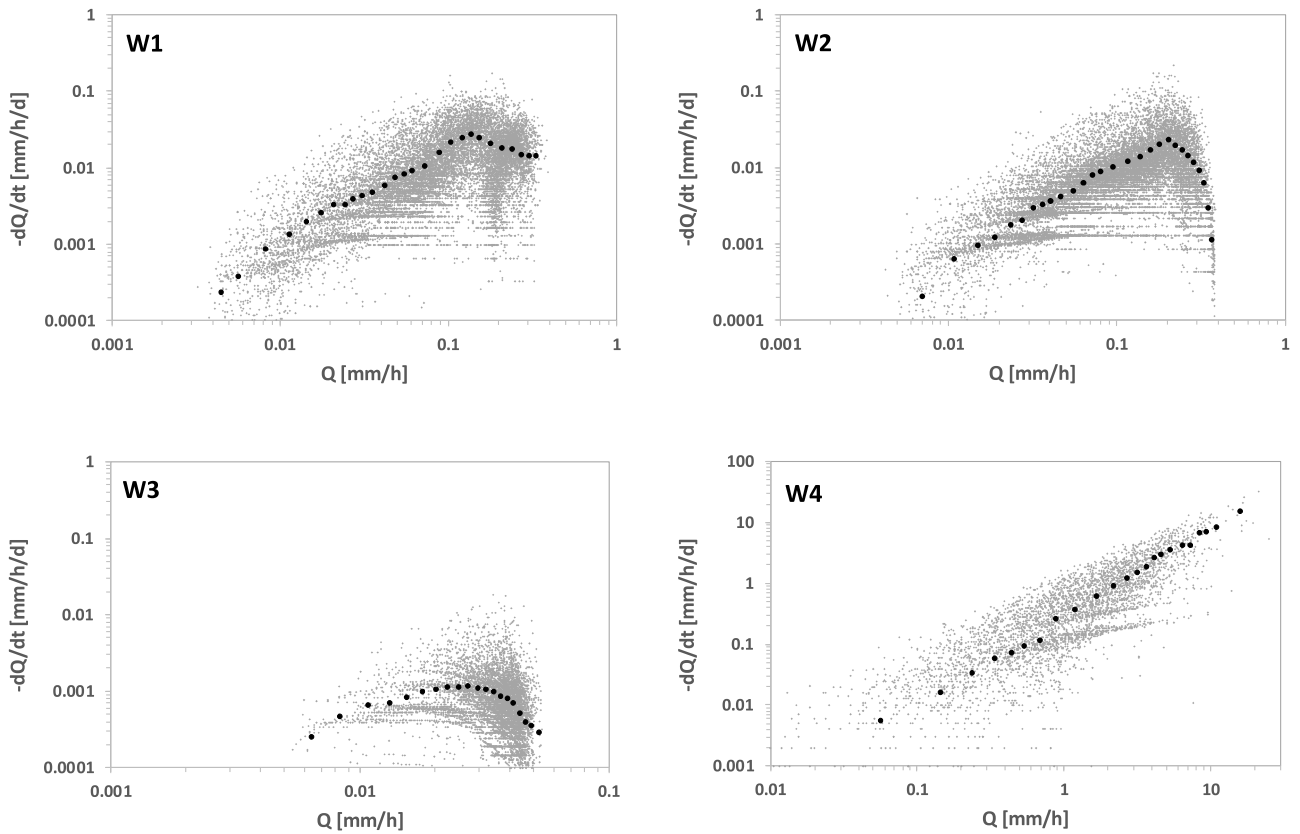


Fig. 4. Recession plots of the karst springs and sinking streams. The black dots are the binned means. Note the differences in the x- and y-axis scale between the stations.

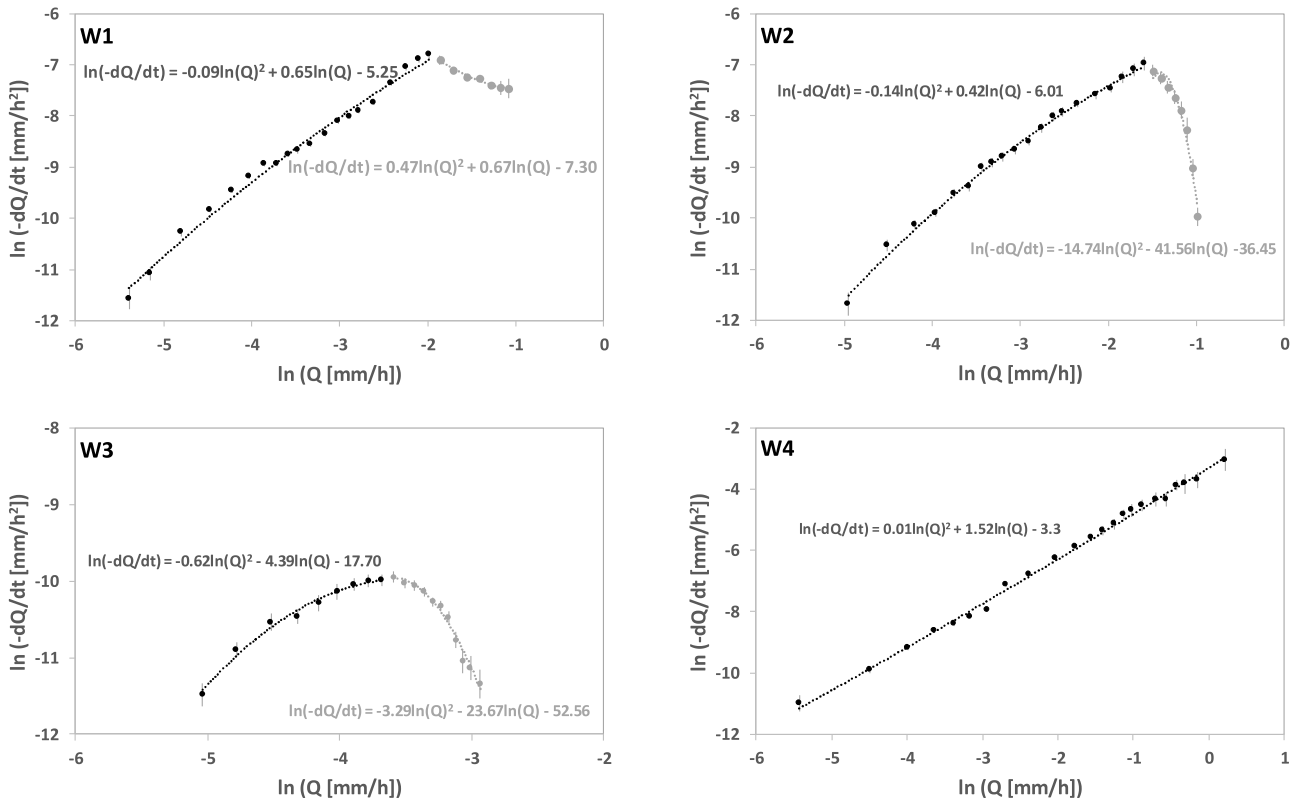


Fig. 5. Binned means (black and gray dots) and their standard errors (gray bars show ± 1 standard error). Dashed curves (black and gray) represent best-fit curves calculated by the least-squares regression with inverse variance weighting.

forms of the curves differ significantly between the stations. The sensitivity functions of stations W1, W2 and W3, respectively, express evident “dual” behavior where recession rates $-dQ/dt$ initially increase with the increasing discharge up to a breaking point where the recession rates start to decline during higher discharges.

The recession dynamics of the karst springs (W1 and W3) and sinking river (W2) cannot be described by a single quadratic curve; therefore, two quadratic curves were used. Similarities in the sensitivity functions’ shape can be seen between the Unica river (W2) and the Ljubljanica river spring (W1) as these two water stations are positioned on the same karst conduit. The sensitivity function of the Cerknjišćica stream (station W4), a karst sinking stream, could be adequately described by a single quadratic function. Most of the sensitivity functions are downward-curving; the exception is the part of the sensitivity function describing the recession rates during high discharges at station W1 and the sensitivity function at station W4 which is slightly upward-curving.

To highlight the seasonal differences in the discharge recession rates, a comparison of the discharge recession rates during selected rainless late autumn and winter periods (the same recession rates as shown in Fig. 5) and discharge recession rates during rainless summer periods (June to August) is shown in Fig. 6. The separation on the late autumn/winter periods and summer periods is based on the observed differences in the seasonal reference ET shown in Fig. 2.

There is an evident increase in the difference between the late autumn/winter and summer recession rates with increasing discharge at station W1, W2 and W4. However, the difference is mainly within the range of the 95% confidence intervals of the sensitivity functions regression curves for the late autumn/winter used in the discharge simulations. During low to medium discharge conditions, the seasonal differences in the recession rates become negligible indicating that the seasonal ET changes might have a highly limited effect on the discharge recession rates during low-flow conditions. Interestingly, very small differences between winter and summer discharge recession rates could

be observed at station W3 for the whole range of observed discharge conditions.

4.2. Discharge simulations

Continuous hourly discharge simulations were performed for individual years in the period 2012–2017. Fig. 7 presents the simulation results for selected karst springs and sinking karst streams. For water stations W1, W2 and W4, the simulation results for 2016 are shown, for the Malenšćica spring (station W3) simulations for 2017 are presented due to limited hourly discharge data availability. Simulation results are summarized in Table 2. The evapotranspiration scaling parameter k_{ET} values ranged between 0.34 and 0.69. The mass conservation ratio “ r ” values ranged between 0.38 and 0.85. The lowest values of “ r ” were calibrated for the Malenšćica spring (station W3), the highest values were calibrated for the Unica river (station W2). The NSE simulation performance criteria ranged between 0.42 and 0.94, NSE_{ln} was between 0.24 and 0.71 (Table 2). Best simulation results were obtained for the Unica river (station W2), NSE was generally above 0.8. The worst simulation results were obtained for the Cerknjišćica sinking stream (station W4), NSE ranged between 0.42 and 0.72 (NSE_{ln} values between 0.18 and 0.49). The simulation results were somewhat worse for years when there was more precipitation in the form of snow as our simple model is not able to consider the possible effect of modified (delayed) runoff formation dynamics due to snowmelt. The snow depth or snow cover characteristics are not systematically monitored in the catchment; generally, the precipitation in the form of snow has considerably diminished in the last few decades. According to the cross-correlation results, the characteristic lag-time for the Cerknjišćica sinking stream was around 6 h, the longest lag-times were defined for station W3 (18-hour lag-time). One should note that the differences in the discharges (expressed in mm/h) are high as the sizes of the catchment area and the discharges range vary greatly between the stations. Station W3 (the

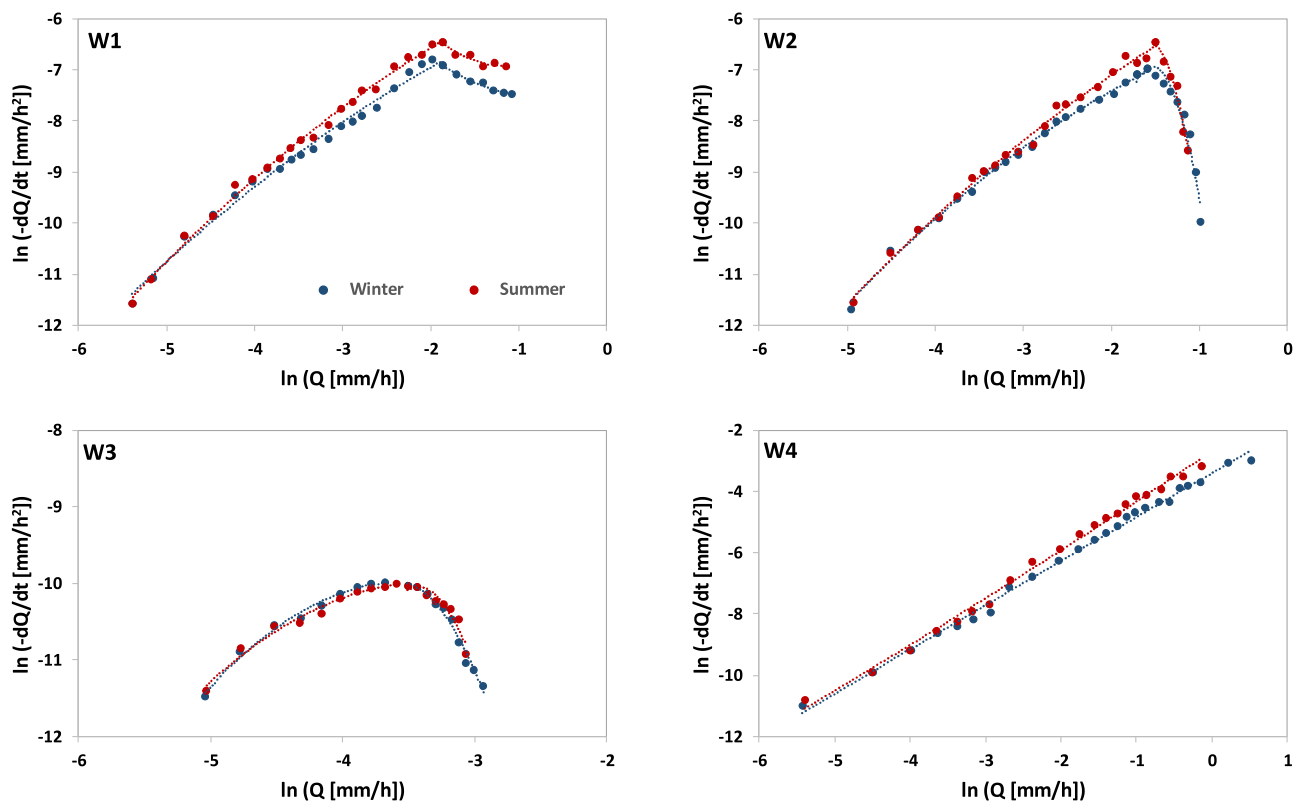


Fig. 6. A comparison of the discharge recession rates during selected rainless late autumn and winter periods (November to February) and discharge recession rates during rainless summer periods (June to August).

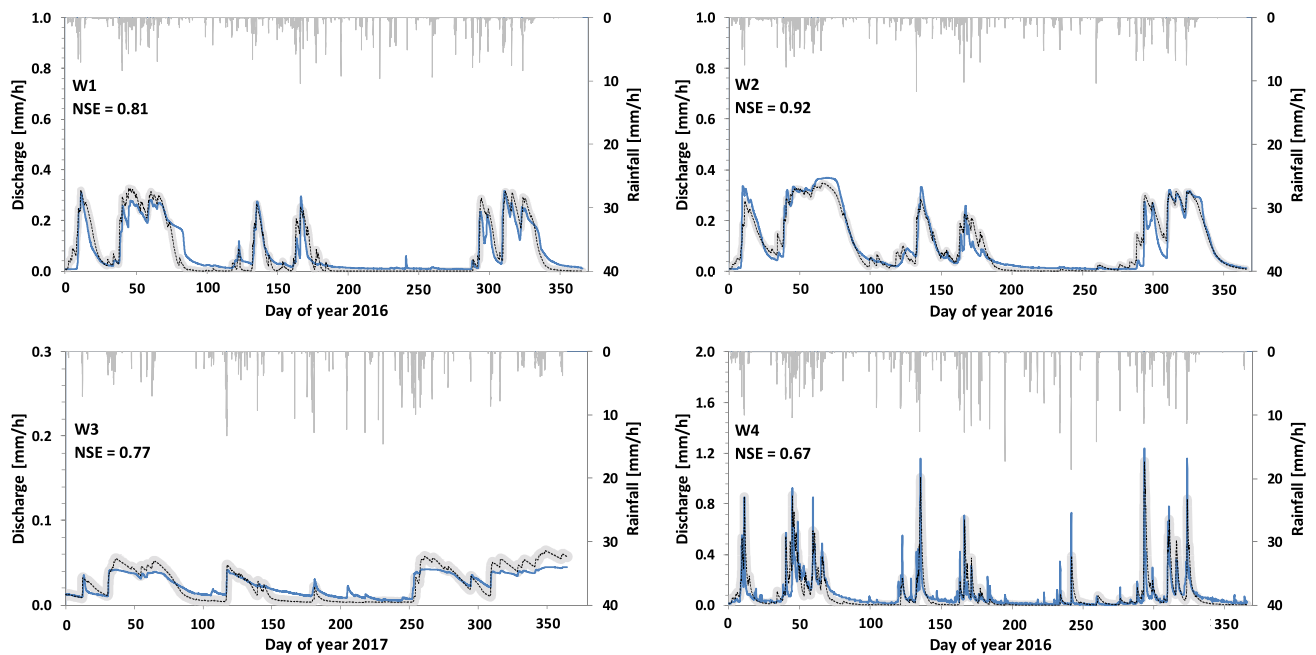


Fig. 7. Discharge simulation results for the selected karst springs and sinking streams. Hourly rainfall rates (gray columns), simulated (dashed black curves), and measured (solid blue curves) hourly discharge time series. The Nash-Sutcliffe efficiency is shown for each simulation period. Thin gray shadowed areas represent the simulation’s 95% uncertainty intervals defined from the confidence intervals of the sensitivity function regression curves. Summer period (day of year No. 152 to 243); Late autumn and winter period (day of year No. 305 to 59).

Table 2
Summary of discharge simulation results.

Location	Name	Lag-time [h]	k_{ET}	r	NSE	NSE_{In}
W1	Vrhnika	15	0.34–0.68	0.58–0.74	0.64–0.87	0.24–0.63
W2	Unica Hasberg	12	0.42–0.65	0.67–0.85	0.76–0.94	0.36–0.71
W3	Malenščica	18	0.38–0.56	0.38–0.51	0.58–0.77	0.20–0.56
W4	Cerkniščica	5	0.46–0.69	0.45–0.56	0.42–0.72	0.18–0.49

Malenščica spring) discharges expressed in mm/h are very small compared to the other stations. The extent of the Malenščica spring catchment area defined by the tracer tests is relatively large in view of the spring discharge which is heavily constrained by the hydraulic conductivity of underground karst system (Table 1).

Generally, the discharge simulations reproduce the observed hydrographs better during high discharge conditions in dormant (late autumn and winter) periods. The low-flow (summer) periods are less well reproduced, even though the overall performance of the simulations for individual years is reasonably good overall in view of the NSE values. However, the NSE_{In} values (Table 2) clearly disclose worse model performance during low-flow conditions. Fig. 8 shows simulation results for station W3 (Malenščica spring) in log-space where evident discrepancies between the measured and modelled discharges can be seen. Similar results could be observed also at other studied karst springs and sinking streams during low-flow periods.

5. Discussion

5.1. Sensitivity functions in view of karst springs and sinking streams catchment area characteristics

As seen from Fig. 7 and the results summarized in Table 2, sensitivity functions derived from long-term daily discharge observations can be relatively successfully used to model hourly discharges in a complex karst catchment. The model performance is comparable and even outperforms some of other, more highly parameterized hydrological

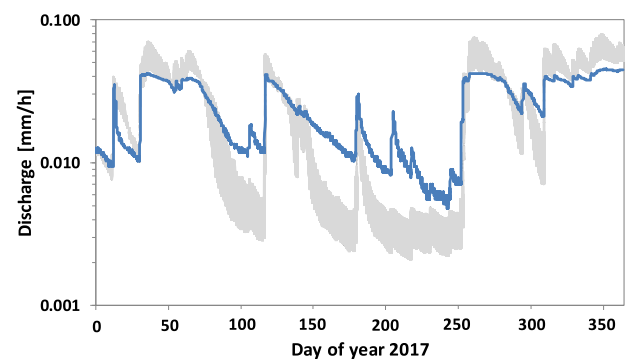


Fig. 8. Simulated (dashed gray curves) and measured (solid blue curves) hourly discharge time series for station W3 (Malenščica spring) in log-space. Gray shadowed areas represent 95% uncertainty intervals calculated from confidence intervals of the sensitivity function regression curves.

modeling tools used in the Ljubljana river catchment (Sezen et al., 2018, 2019) where the inclusion of additional meteorological variables did not significantly improve the modeling results. The simulation results indicate that the model is generally able to satisfactorily follow the discharge increases (i.e., karst storage recharge events) and also the hydrograph formation during the peak discharges. During early phases of recharge periods, the formation of the hydrographs is closely related to flow formation along the preferential conduits. The sensitivity

functions can well represent the link between the karst underground catchment storage mainly controlled by the karst underground conduits hydraulic conveyance, and the karst spring discharge response during medium to high discharge conditions. Kaufmann et al. (2020) presented a process-based modeling approach of the karst conduit system in one part of the studied catchment, concentrating on the discharge distribution between the Malenščica spring (W3) and the neighboring Unica spring. Since our approach concentrates on the aggregated response of the studied karst springs/sinking stream, it is not able to distinguish specific karst conduit hydraulic characteristics; however, some interesting parallels with the findings by (Kaufmann et al., 2020) could be drawn. The W3 spring discharge is strongly controlled by the baseflow conduit with a limited hydraulic conveyance; during the increased flow conditions this causes redirection of the high discharges over the underground overflow breakdown towards the neighboring underground conduit branches. The W3 karst system could be characterized by conduit influenced flow regime according to the quantitative method by Kovacs et al. (2005). The damping effect of the W3 baseflow conduits is clearly reflected in the specific shape of the W3 discharge sensitivity function with a strong decrease in the discharge recession rates during high discharges when the underground conduit system reaches its peak hydraulic conveyance.

However, as in the case of many hydrological models, the discharge simulations based on the derived sensitivity functions perform well in wet conditions, but worse during dry conditions which is evident from the NSE_{in} values. The main causes for worse simulation results in the summer and during low-flow conditions could be related especially to the following factors: (1) Uneven spatial distribution of rainfall during summer storms over the catchment area which cannot be properly accounted for by the available rainfall station data and the consequent Thiessen polygon spatial rainfall interpolation. It is expected that the simulations would perform better on smaller spatial scales where the rainfall is more spatially homogeneous. (2) The inability to properly account for low discharge recession dynamics at water stations during low-flow conditions (high scatter in discharge recession rates shown in Fig. 4 and no “detectable” change in the discharge between the consecutive daily records). This reflects in the saw-shape measured discharge recession during low-flow periods (Fig. 8). Water resource management of karst aquifers will undoubtedly need improved tools to analyze discharge recession during low-flow conditions, especially in view of the future climate change impact on the water availability (Sapač et al., 2020; Olanoye et al., 2022). A possible way forward to improve the implementation of the methodology for simulating low-flow conditions in heterogeneous karst catchments could be to derive a specific discharge sensitivity function that would better describe the extremely slow and scattered discharge recession rates. (3) The influence of evapotranspiration in the summer periods. Negligible differences in the discharge recession rates between dormant and summer periods could be detected at all stations during the low-flow conditions (Fig. 6), which indicate that the seasonal ET changes might have a highly limited effect on the discharge recession rates during low-flow conditions. Therefore, the seasonal impact of ET on the simulated recession rates could be reduced for low-flow conditions, in our simulations this could be done by adjusting the k_{ET} parameter. Especially interesting is the discharge recession behavior at station W3 which appears to be seasonally relatively independent for the whole range of the discharge conditions. Intensive percolation of rainfall through highly fissured epikarst towards deep karst aquifer of the station W3 apparently makes the spring discharge recession relatively isolated from the seasonal influence (e.g. of ET) on the discharge recession rates. Additionally, the hydrological homogenization of the karst catchment response along the preferential karst conduits might contribute to melioration of high spatial variability in precipitation inputs and also the influence of seasonally and spatially variable evapotranspiration as indicated by the water stable isotope composition (Riechelmann et al., 2017; Domínguez-Villar et al., 2018).

The shape of catchment sensitivity functions could be used to analyze the karst spring and sinking stream characteristics, which often change abruptly depending on the preceding hydrological conditions. This is evident from studied karst springs and sinking streams sensitivity function shapes, which vary considerably (Fig. 5). The W1 and W2 stations' sensitivity function shapes describing the discharge recession during low-flow conditions up to the maximum discharge recession rates (black dotted curves in Fig. 5) are rather similar. The black curves cover the range of discharges, which flow relatively freely along the karst underground conduits separating the two stations. On the other hand, there are considerable differences in the sensitivity function shapes describing the decrease in the discharge recession rates during high-flow conditions (discharges higher than the binned mean discharge with the highest recession rates, gray curves in Fig. 5). The decrease in the discharge recession rates at station W1 is much smaller than the decrease in the recession rates at station W2. Namely, station W2 is positioned in the Planinsko polje, which becomes flooded several times each year. The Planinsko polje is a typical karst polje in Slovenia, the flooding of the Planinsko polje can last for a few months, the volume of the stored water can exceed 80 million m^3 (Frantar and Ulaga, 2014). A sharp decrease in the discharge recession rates is a result of slow emptying of the karst polje after extensive flood events. The emptying of the Planinsko karst polje is regulated by the hydraulic conductivity of the polje's ponors and underground karst conduits further downstream towards station W1. The effect of the slow emptying of Planinsko polje when the depression polje area stores large amount of water, can be seen also from measured hydrographs at stations W1 and W2 in Fig. 7 during spring and fall hydrographs when hydrograph plateauing is visually evident. When the Planinsko polje dries out, the discharge recession increases considerably. The simulated hydrographs (dashed black curves in Fig. 7) are not able to fully capture such phenomena.

The sensitivity function of water station W3 (Malenščica spring) is heavily downward-curved and shows a much smaller variability in discharge recession compared to other stations (Fig. 5). Interestingly, during extremely high and extremely low discharges, the discharge recession rates are almost the same, in log values less than -11 mm/h^2 (Fig. 5). The unusual sensitivity function shape could be related to the complex Malenščica spring recharge dynamics which depends on the hydrological conditions. During steady low-flow conditions, the heavily fissured and porous Javorniki karst area with its deep karst aquifer is the dominant drainage area. In periods of increased water pulses, the recharge from the Cerknica part of the catchment controlled by the water levels in intermittent Lake Cerknica becomes important (Petrič, 2010; Ravbar et al., 2012). A strong decrease in the Malenščica spring discharge recession during high flows could be related to strong damping of the karst underground conduits hydraulic conveyance, relatively constant water levels from the direction of Lake Cerknica and the influence of the Mysterious Lake discussed by Kaufmann et al. (2020), which act as a hydraulic boundary condition for the flow through the underground karst conduits.

The sensitivity function for station W4 (Cerkniščica intermittent sinking stream) expresses almost a linear discharge recession increase with the increasing discharge. The Cerkniščica stream collects water mainly from the local surface and near-surface flows, which reflects in a more abrupt, almost torrential response to precipitation and a much faster discharge recession compared to other stations; this can be seen from hydrographs in Fig. 7.

5.2. Dynamic karst catchment storage

Sensitivity functions express the sensitivity of discharge to changes in the catchment storage and can be further used to explore the karst catchment storage characteristics. Integrating the storage-discharge relationships results in hypothetical recession curves (discharge as a function of time) that can be used to study how fast the discharges from karst springs and sinking streams recede in a theoretical case when there

is no rainfall and the influence of evapotranspiration is neglected. The recession curves derived for the studied karst springs and sinking streams are shown in Fig. 9. Significant differences in the discharge recession dynamics can be distinguished. The recession curves' shapes indicate the presence of breaking points (the only exception is the station W4 recession curve) which most probably results from the changes in the flow regime throughout the karst storages (e.g. emptying of the surface karst depressions or karst caves during high-flow conditions and variability in the micro-regime flow throughout the karst aquifer due to the changes in the fissure system), similarly as suggested by Bonacci (1993). Many of the karst springs recession curves that can be found in the literature were obtained by using the pre-defined equation form (e.g. such as the one proposed by Maillet (1905)) and fit the equation parameters to separate recession curve segments. In our case, the recession curves were derived directly from the discharge recession data.

If, theoretically, one would let the karst spring/sinking stream discharges to recede from discharge maximum recorded values to discharge minimum recorded values (normalized discharge values shown on y axis in Fig. 9) following the derived recession curves, the W1 spring (Vrhnika) discharge would drop to its minimum values in approx. 50 days and the W2 sinking river (Unica) in 75 days. The fastest would be the recession of the intermittent sinking stream W4 (intermittent Cerknjšičica stream) whose discharge would drop to its minimum values after approx. 30 days. The slowest would be the recession of spring W3 where the theoretical recession down to the minimum discharge would take approx. 80 days. The theoretical recession duration for water stations W2 and W3 are rather similar when the discharge recedes to extremely low values as most of the discharge at station W2 comes from spring W3 during dry conditions. The comparison of summer and winter discharge recession curves (Fig. 9) for each water station discloses some interesting seasonal differences. The differences in the shape of the discharge recession curves are smaller during high-discharge conditions, then the difference somewhat increases in the range of mean discharge conditions and becomes very small during low-flow conditions.

During flood periods, the discharge of the selected karst springs and sinking streams is heavily constrained by the hydraulic conveyance of the karst underground conduits as clearly seen from the shapes of the catchment sensitivity functions (the only exception being station W4). This indicates the evident "dual" behavior of the karst catchment storage (Fig. 5). In periods of extensive rainfall events, the sinks in the karst poljes (Planinsko polje and intermittent Lake Cerknica) regulate the discharge regime. These karst depressions consequently become flooded when the hydraulic conductivity of the karst underground conduits becomes exceeded. This is indicated by an evident decrease in the discharge recession rates during high-flow conditions (part of the sensitivity functions described by the gray curves in Fig. 5). Further, this

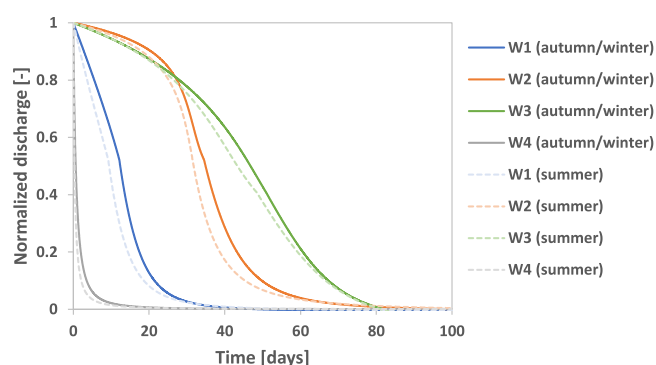


Fig. 9. Comparison of the discharge recession curves for the studied karst springs and sinking streams for the late autumn/winter and summer periods. The values on the y axis are normalized discharges calculated by considering a range of discharge values between maximum (value of 1 on y axis) and minimum (value of 0 on y axis) recorded discharges at each station.

leads to a considerable increase in the total catchment water storage, especially the catchment surface storage as the karst poljes act as natural surface flood water detention areas (Kranjc, 1985; Frantar and Ulaga, 2014).

The sensitivity functions offer the possibility to analyze the characteristics of the dynamic karst catchment storage characterized as storage variability between dry and wet periods. The water detention capacity of karst aquifers can be in some karst areas relatively limited (Bonacci, 1993, 2001). The extent of the dynamic karst underground storage remains one of the main unknowns in the karst catchment hydrology and provides important information for many water management issues (Einsiedl, 2005; Butscher and Huggenberger, 2008; McNamara et al., 2011; Hartmann et al., 2013; Mudarra et al., 2019), such as the sustainability of low flows for different water abstraction purposes during prolonged rainless periods. Abirifard et al. (2022) demonstrated how different parameters used for simulating the karst spring recession affect the accuracy of the hypothetical karst aquifer dynamic volume. They highlighted the importance of integral information that the discharge recession provides on the characteristics of the entire karst storage, which includes summed effects of spatio-temporal distribution of recharge, the hydraulic characteristics of the different compartments of the karst matrix (i.e. epikarst, vadose and phreatic zones) as well as the effect of flow partitioning between highly permeable and less permeable zones. Cinkus et al. (2021) proposed a classification for karst systems which, based on the karst springs' discharges series, distinguishes their capacity of dynamic storage, the draining dynamic of their capacitive function and the variability of their hydrological functioning. We assume that the dynamic storage could be primarily described by the part of the total karst catchment sensitivity function represented by the black dotted curve in Fig. 5. This part of the total catchment sensitivity function, which describes the discharge recession rates from low-flow conditions up to the discharge with maximum discharge recession rates, could be therefore suitable for investigation of the dynamic karst underground storage during hydrological conditions when the main karst underground conduits hydraulic conveyance is not considerably exceeded. We described the dynamic storage for the selected discharge range (black dotted curves in Fig. 5) by integrating the reciprocal of the sensitivity function. The resulting storage-discharge relationships for the selected karst springs and sinking streams are shown in Fig. 10. Since sections of the sensitivity functions described by the black curves in Fig. 5 was used, the storage-discharge relationship is valid up to the discharges indicated by the black dashed horizontal arrows (Q_{max} in Fig. 10 which represents the discharge with a maximum discharge recession rate). The gray dashed arrows indicate the long-term minimal daily discharge at the selected station (Q_{min} in Fig. 10). The storage-discharge relationship for higher discharges (where the discharge recession rates decrease, data described by gray curves in Fig. 5) leads to a fast increase in the storage with an increasing discharge. The difference between the storage levels at discharge rates Q_{min} and Q_{max} could be used to estimate the size of dynamic karst catchment storage. Since the sensitivity functions cannot provide information on the absolute levels of the storage, storage measures on x axis in Fig. 10 are shown as storage relative to the storage at mean discharge.

The sizes of the relative dynamic storage for stations W1 and W2 are 8 mm and 12 mm, respectively. Station W3 has very small relative dynamic storage. The Malenjšičica karst spring has a relatively constant discharge and a very small variability in discharge. The discharge is controlled by the flow from the phreatic zone spreading over extensive, highly karstified part of the catchment. The thick fissured epikarst and vadose zones in the Javorniki area, divert the excess water during high discharges towards the neighboring intermittent karst springs and streams causing the discharge and the dynamic storage at the Malenjšičica spring to vary by a much smaller extent. Additionally, the relatively constant discharge indicates a considerable and stable residual storage. This could be confirmed through the stable isotopes monitoring where

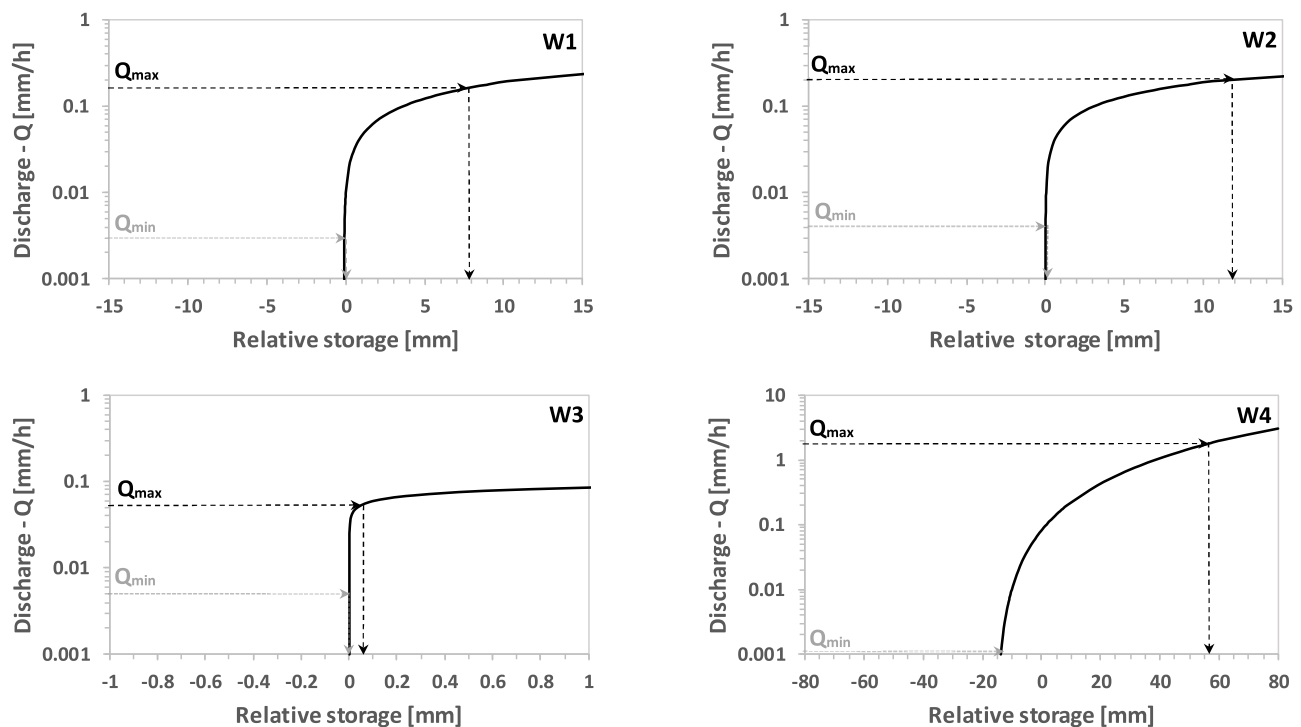


Fig. 10. The storage-discharge relationship for the selected karst springs and sinking streams. The relationship is valid up to the max. discharge (Q_{max}) indicated by the black dashed horizontal arrows. Note the differences in the x axis ranges between the various stations. The storage measures on x axis are relative to the storage at mean discharge.

the water from the Malenščica spring was found to have the longest mean residence time among the neighboring karst springs and sinking streams (Rusjan et al., 2019). Further, the analysis of several low-flow indices of the Malenščica spring indicated very limited seasonal influence on the low-flows recession dynamics (Sapač et al., 2020). All these characteristics make the Malenščica spring an ideal source for water abstraction. The highest relative dynamic storage of approx. 70 mm was assessed at the intermittent Cerknjšica stream (station W4) which has a torrential discharge regime. The Cerknjšica stream catchment residual water storage appears to be small as the stream dries out during prolonged rainless periods.

6. Conclusion

In our study we implemented a modified dynamical system approach in a highly heterogeneous karst catchment, where the hydrogeological characteristics and the resulting discharge temporal dynamics vary greatly among the neighboring karst springs and sinking streams. We have shown that important information about the karst catchment areas discharge-storage relationship can be extracted from the long-term discharge data, which are usually available on a coarser time step, in our case daily data. The implemented approach offers a high potential for advancement in karst hydrology, especially since discharge data, such as the ones used in our study, present the basis for analyzing karst system characterization, which has been traditionally used to investigate the integrated karst catchment behavior at major karst springs. The main advantage of the proposed approach is that the discharge recession data can be used in a straightforward way. The discharge recession is derived directly by the statistical fit, additional pre-defined theoretical equations which are in many cases applied to describe the discharge recession dynamics of karst springs are not needed. Despite the considerable differences in the sensitivity function shapes of the karst springs and sinking streams as a result of diverse karst hydrogeological characteristics, the functions can be successfully used for discharge simulations and characterization of the storage-discharge relationships.

The main drawback of the proposed approach is the limited ability of the derived discharge sensitivity functions to describe the complexity of the heterogeneous karst storage during low-flow conditions. Additionally, the presented approach is not able to consider the fraction of rainfall-runoff which bypasses the underground storage (e.g. overland flow or direct precipitation on wetted areas); however, the proportion of such bypass rainfall-runoff pathways is presumably relatively limited in karst.

Existing karst catchment process knowledge, obtained by various karst exploration techniques (e.g. by measuring hydrochemical parameters and tracer applications), should be combined to guide the development of new data-driven modeling concepts, such as the one implemented in our study. We demonstrated that additional information about the catchment storage can be extracted from the karst springs and sinking streams time series which can be found helpful in karst water resource management; however, further work is needed to test the generality of the approach in karst systems with variable hydrological functioning.

CRediT authorship contribution statement

Simon Rusjan: Funding acquisition, Conceptualization, Formal analysis, Writing – original draft, Writing – review & editing, Visualization. **Klaudija Lebar:** Data curation, Formal analysis, Project administration, Visualization. **Nejc Bezak:** Data curation, Formal analysis, Project administration.

Declaration of Competing Interest

The authors declare the following financial interests/personal relationships which may be considered as potential competing interests:

Simon Rusjan reports financial support was provided by Slovenian Research and Innovation Agency (ARIS). Simon Rusjan reports financial support was provided by Slovenian national commission for UNESCO IHP.

Data availability

Data will be made available on request.

Acknowledgements

The results of this study are part of the Slovenian national research project No. J2–7322 and No. J6–4628 and research program P2–0180 financed by the Slovenian Research and Innovation Agency (ARIS) and co-financed by the Slovenian national commission for UNESCO IHP. We wish to thank the Slovenian Environment Agency for precipitation, evapotranspiration, and discharge data provision. Authors would like to thank three anonymous reviewers for their constructive comments which helped us to improve the paper considerably.

References

- Abbaspour, K.C., Yang, J., Maximov, I., Saber, R., Bogner, K., Mieleitner, J., Zobrist, J., Srinivasan, R., 2007. Modelling hydrology and water quality in the pre-alpine/alpine Thur watershed using SWAT. *J. Hydrol.* 333, 413–430. <https://doi.org/10.1016/j.jhydrol.2006.09.014>.
- Abirifard, M., Birk, S., Raesi, E., Sauter, M., 2022. Dynamic volume in karst aquifers: parameters affecting the accuracy of estimates from recession analysis. *J. Hydrol.* 612, 128286 <https://doi.org/10.1016/j.jhydrol.2022.128286>.
- Adamovic, M., Braud, I., Branger, F., Kirchner, J.W., 2015. Assessing the simple dynamical systems approach in a Mediterranean context: application to the Ardèche catchment (France). *Hydrol. Earth Syst. Sci.* 19, 2427–2449. <https://doi.org/10.5194/hess-19-2427-2015>.
- Atkinson, S.E., Woods, R.A., Sivapalan, M., 2002. Climate and landscape controls on water balance model complexity over changing timescales. *Water Resour. Res.* 38 (12), 1314. <https://doi.org/10.1029/2002WR001487>.
- Birkel, C., Soulsby, C., Tetzlaff, D., 2015. Conceptual modelling to assess how the interplay of hydrological connectivity, catchment storage and tracer dynamics controls nonstationary water age estimates. *Hydrol. Process.* 29 (13), 2956–2969. <https://doi.org/10.1002/hyp.10414>.
- Blatnik, M., Frantar, P., Kosec, D., Gabrovšek, F., 2017. Measurements of the outflow along the eastern border of Planinsko polje, Slovenia. *Acta Carsologica* 46 (1), 83–93. <https://doi.org/10.3986/ac.v46i1.4774>.
- Bonacci, O., 1993. Karst spring hydrographs as indicators of karst aquifers. *Hydrol. Sci. J.* 38, 51–62. <https://doi.org/10.1080/0262666930942639>.
- Bonacci, O., Roje-Bonacci, T., 2000. Interpretation of groundwater level monitoring results in karst aquifers: examples from the Dinaric karst. *Hydrol. Process.* 14 (14), 2423–2438. [https://doi.org/10.1002/1099-1085\(20001015\)14:14<2423::AID-HYP104>3.0.CO;2-2](https://doi.org/10.1002/1099-1085(20001015)14:14<2423::AID-HYP104>3.0.CO;2-2).
- Bonacci, O., 2001. Analysis of the maximum discharge of karst springs. *Hydrogeol. J.* 9, 328. <https://doi.org/10.1007/s100400100142>.
- Bonacci, O., 2004. Hazards caused by natural and anthropogenic changes of catchment area in karst. *Nat. Hazards Earth Syst. Sci.* 4, 655–661. <https://doi.org/10.5194/nhess-4-655-2004>.
- Bonacci, O., Andrić, I., 2015. Karst spring catchment: an example from Dinaric karst. *Environ. Earth Sci.* 74 (7), 6211–6223. <https://doi.org/10.1007/s12665-015-4644-8>.
- Brauer, C.C., Teuling, A.J., Torfs, P.J.J.F., Uijlenhoet, R., 2013. Investigating storage-discharge relations in a lowland catchment using hydrograph fitting, recession analysis, and soil moisture data. *Water Resour. Res.* 49 (7), 4257–4264. <https://doi.org/10.1002/wrcr.20320>.
- Butscher, C., Huggenberger, P., 2008. Intrinsic vulnerability assessment in karst areas: a numerical modeling approach. *Water Resour. Res.* 44 (3), W03408. <https://doi.org/10.1029/2007WR006277>.
- Cinkus, G., Mazzilli, N., Jourde, H., 2021. Identification of relevant indicators for the assessment of karst systems hydrological functioning: proposal of a new classification. *J. Hydrol.* 603, 127006.
- Chen, Z., Hartmann, A., Wagener, T., Goldscheider, N., 2018. Dynamics of water fluxes and storages in an Alpine karst catchment under current and potential future climate conditions. *Hydrol. Earth Syst. Sci.* 22, 3807–3823. <https://doi.org/10.5194/hess-22-3807-2018>.
- Dewandel, B., Lachassagne, P., Bakalowicz, M., Weng, P., Al-Malki, A., 2003. Evaluation of aquifer thickness by analysing recession hydrographs. Application to the Oman ophiolite hard-rock aquifer. *J. Hydrol.* 274, 248–269. [https://doi.org/10.1016/S0022-1694\(02\)00418-3](https://doi.org/10.1016/S0022-1694(02)00418-3).
- Domínguez-Villar, D., Lojen, S., Krklec, K., Kozdon, R., Edwards, R.L., Cheng, H., 2018. Ion microprobe $\delta^{18}O$ analyses to calibrate slow growth rate speleothem records with regional $\delta^{18}O$ records of precipitation. *Earth Planet. Sci. Lett.* 482, 367–376. <https://doi.org/10.1016/j.epsl.2017.11.012>.
- Efstratiadis, A., Koutsoyiannis, D., 2010. One decade of multi-objective calibration approaches in hydrological modelling: a review. *Hydrol. Sci. J.* 55 (1), 58–78. <https://doi.org/10.1080/02626660903526292>.
- Einsiedel, F., 2005. Flow system dynamics and water storage of a fissured-porous karst aquifer characterized by artificial and environmental tracers. *J. Hydrol.* 312 (1–4), 312–321. <https://doi.org/10.1016/j.jhydrol.2005.03.031>.
- Fiorillo, F., 2014. The recession of spring hydrographs, focused on karst aquifers. *Water Resour. Manag.* 28, 1781–1805. <https://doi.org/10.1007/s11269-014-0597-z>.
- Ford, D., Williams, P.W., 2007. *Karst Hydrogeology and Geomorphology*. Wiley, Chichester. <https://doi.org/10.1002/9781118684986>.
- Frantar, P., Ulaga, F., 2014. High waters at the Planinsko polje in 2014. *Ujma* 29, 66–73.
- Gabrovšek, F., Kogovšek, J., Kovacič, G., Petrič, M., Ravbar, N., Turk, J., 2010. Recent results of tracer tests in the catchment of the Unica River (SW Slovenia). *Acta Carsologica* 39 (1), 27–37. <https://doi.org/10.3986/ac.v39i1.110>.
- Gams, I., 1970. Underground discharge maximums in the area between Cerknica and Planina polje. *Acta Carsologica* 5, 171–187 (in Slovene).
- Ghasemzadeh, R., Hellweger, F., Butscher, C., Padilla, I., Vesper, D., Field, M., Alshwabkeh, A., 2012. Review: groundwater flow and transport modeling of karst aquifers, with particular reference to the North Coast Limestone aquifer system of Puerto Rico. *Hydrogeol. J.* 20, 1441–1461. <https://doi.org/10.1007/s10040-012-0897-4>.
- Gospodarič, R., Habič, P., 1976. *Underground water tracing: investigations in Slovenia 1972-1975*. In: *Proceedings of the third international symposium of underground water tracing (3. SUWT)*. Ljubljana, Bled.
- Hartmann, A., Barberá, J.A., Lange, J., Andreo, B., Weiler, M., 2013. Progress in the hydrologic simulation of time variant recharge areas of karst systems—Exemplified at a karst spring in Southern Spain. *Adv. Water Resour.* 54, 149–160. <https://doi.org/10.1016/j.advwatres.2013.01.010>.
- Hartmann, A., Goldscheider, N., Wagener, T., Lange, J., Weiler, M., 2014. Karst water resources in a changing world: review of hydrological modeling approaches. *Rev. Geophys.* 52, 218–242. <https://doi.org/10.1002/2013RG000443>.
- Hartmann, A., Gleeson, T., Wada, Y., Wagener, T., 2017. Enhanced groundwater recharge rates and altered recharge sensitivity to climate variability through subsurface heterogeneity. *Proceedings of the National Academy of Sciences* 114 (11), 2842–2847. <https://doi.org/10.1073/pnas.1614941114>.
- Kaufmann, G., Mayaud, C., Kogovšek, B., Gabrovšek, F., 2020. Understanding the temporal variation of flow direction in a complex karst system (Planinska Jama, Slovenia). *Acta Carsologica* 49 (2–3). <https://doi.org/10.3986/ac.v49i2-3.7373>.
- Kavetski, D., Fenicia, F., Clark, M.P., 2011. Impact of temporal data resolution on parameter inference and model identification in conceptual hydrological modeling: insights from an experimental catchment. *Water Resour. Res.* 47 (5), W05501. <https://doi.org/10.1029/2010WR009525>.
- Király, L., 2002. Karstification and groundwater flow. In: *Postojna-Ljubljana, Gabrovšek, F. (Eds.), Evolution of karst: from Prekarst to Cessation*. Založba ZRC, pp. 155–190.
- Kirchner, J.W., 2009. Catchments as simple dynamical systems: catchment characterization, rainfall-runoff modeling, and doing hydrology backward. *Water Resour. Res.* 45 (2), W02429. <https://doi.org/10.1029/2008WR006912>.
- Kogovšek, J., Petrič, M., 2010. Water temperature as a natural tracer: a case study of the Malenšička karst spring (SW Slovenia). *Geologia Croatica* 63 (2), 171–177. <https://doi.org/10.4154/gc.2010.14>.
- Kogovšek, J., Petrič, M., 2014. Solute transport processes in a karst vadose zone characterized by long-term tracer tests (the cave system of Postojnska Jama, Slovenia). *J. Hydrol.* 519, 1205–1213. <https://doi.org/10.1016/j.jhydrol.2014.08.047>.
- Kovács, A., Perrochet, P., Király, L., Jeannin, P.Y., 2005. A quantitative method for the characterisation of karst aquifers based on spring hydrograph analysis. *J. Hydrol.* 303 (1–4), 152–164. <https://doi.org/10.1016/j.jhydrol.2004.08.023>.
- Kranjc, A., 1985. *Cerknica lake and its floods (in Slovene)*. Geografski Inštitut Antona Melika. ZRC SAZU.
- Kresic, N., 2007. *Hydrogeology and Groundwater Modeling*, 2nd edn. CRC Press/Taylor&Francis, Boca Raton, p. 807. <https://doi.org/10.1201/9781420004991>.
- Kresic, N., Stevanovic, Z., 2009. *Groundwater Hydrology of Springs: Engineering, Theory, Management and Sustainability*. Butterworth-Heinemann, Oxford, U. K. <https://doi.org/10.1016/C2009-0-19145-6>.
- Krklec, K., Domínguez-Villar, D., Lojen, S., 2018. The impact of moisture sources on the oxygen isotope composition of precipitation at a continental site in central Europe. *J. Hydrol.* 561, 810–821. <https://doi.org/10.1016/j.jhydrol.2018.04.045>.
- Liu, M., Xu, X., Sun, A.Y., Luo, W., Wang, K., 2018. Why do karst catchments exhibit higher sensitivity to climate change? Evidence from a modified Budyko model. *Adv. Water Resour.* 122, 238–250. <https://doi.org/10.1016/j.advwatres.2018.10.013>.
- Maillet, E., 1905. *Essais D'hydraulique Souterraine Et Fluviale [Underground and River Hydrology]*. Hermann, Paris, p. 218.
- Maneta, M.P., Soulsby, C., Kuppel, S., Tetzlaff, D., 2018. Conceptualizing catchment storage dynamics and nonlinearities. *Hydrol. Process.* 32 (21), 3299–3303. <https://doi.org/10.1002/hyp.13262>.
- Mazzilli, N., Guinot, V., Jourde, H., 2012. Sensitivity analysis of conceptual model calibration to initialisation bias. Application to karst spring discharge models. *Adv. Water Resour.* 42, 1–16. <https://doi.org/10.1016/j.advwatres.2012.03.020>.
- McMahon, T.A., Peel, M.C., Lowe, L., Srikanthan, R., McVicar, T.R., 2013. Estimating actual, potential, reference crop and pan evaporation using standard meteorological data: a pragmatic synthesis. *Hydrol. Earth Syst. Sci.* 17, 1331–1363. <https://doi.org/10.5194/hess-17-1331-2013>.
- McNamara, J.P., Tetzlaff, D., Bishop, K., Soulsby, C., Seyfried, M., Peters, N.E., Aulenbach, B.T., Hooper, R., 2011. Storage as a metric of catchment comparison. *Hydrol. Process.* 25 (21) <https://doi.org/10.1002/hyp.8113>.
- Mudarra, M., Hartmann, A., Andreo, B., 2019. Combining Experimental Methods and Modeling to Quantify the Complex Recharge Behavior of Karst Aquifers. *Water Resour. Res.* 55 (2), 1384–1404. <https://doi.org/10.1029/2017WR021819>.
- Olariño, T., Gleeson, T., Hartmann, A., 2022. Karst spring recession and classification: efficient, automated methods for both fast-and slow-flow components. *Hydrol. Earth Syst. Sci.* 26 (21), 5431–5447. <https://doi.org/10.5194/hess-26-5431-2022>.

- Petrič, M., 2010. Characterization, exploitation, and protection of the Malenščica karst spring, Slovenia. In: Kresic, N., Stevanovic, Z. (Eds.), *Groundwater Hydrology of springs. Engineering, theory, management, and Sustainability*. Butterworth-Heinemann, Oxford, pp. 428–441.
- Petrič, M., Kogovšek, J., Ravbar, N., 2018. Effects of the vadose zone on groundwater flow and solute transport characteristics in mountainous karst aquifers – the case of the Javorniki–Snežnik massif (SW Slovenia). *Acta Carsologica* 47 (1), 35–51. <https://doi.org/10.3986/ac.v47i1.5144>.
- Ravbar, N., Engelhardt, L., Goldscheider, N., 2011. Anomalous behaviour of specific electrical conductivity at a karst spring induced by variable catchment boundaries: the case of the Podstenjšek spring, Slovenia. *Hydrol. Process.* 25 (3), 2130–2140. <https://doi.org/10.1002/hyp.7966>.
- Ravbar, N., Barberá, J.A., Petric, M., Kogovsek, J., Andreo, B., 2012. The study of hydrodynamic behaviour of a complex karst system under low-flow conditions using natural and artificial tracers (the catchment of the Unica River, SW Slovenia). *Environ. Earth Sci.* 65 (8), 2259–2272. <https://doi.org/10.1007/s12665-012-1523-4>.
- Riechelmann, S., Schröder-Ritzrau, A., Spötl, C., Riechelmann, D.F.C., Richter, D.K., Mangini, A., Frank, N., Breitenbach, S.F.M., Immenhauser, A., 2017. Sensitivity of Bunker Cave to climatic forcings highlighted through multi-annual monitoring of rain-, soil-, and dripwaters. *Chem. Geol.* 449, 194–205. <https://doi.org/10.1016/j.chemgeo.2016.12.015>.
- Rusjan, S., Mikoš, M., 2015. A catchment as a simple dynamical system: characterization by the streamflow component approach. *J. Hydrol.* 527, 794–808. <https://doi.org/10.1016/j.jhydrol.2015.05.050>.
- Rusjan, S., Sapač, K., Petrič, M., Lojen, S., Bezak, N., 2019. Identifying the hydrological behavior of a complex karst system using stable isotopes. *J. Hydrol.* 577, 123956 <https://doi.org/10.1016/j.jhydrol.2019.123956>.
- Sapač, K., Rusjan, S., Šraj, M., 2020. Assessment of consistency of low-flow indices of a hydrogeologically non-homogeneous catchment: a case study of the Ljubljana river catchment, Slovenia. *J. Hydrol.* 583, 124621 <https://doi.org/10.1016/j.jhydrol.2020.124621>.
- Schmidt, S., Geyer, T., Guttman, J., Marei, A., Ries, F., Sauter, M., 2014. Characterisation and modelling of conduit restricted karst aquifers – example of the Auja spring, Jordan Valley. *J. Hydrol.* 511 <https://doi.org/10.1016/j.jhydrol.2014.02.019>.
- Sezen, C., Bezak, N., Šraj, M., 2018. Hydrological modelling of the karst Ljubljana River catchment using lumped conceptual model. *Acta hydrotechnical* 31 (55), 87–100. <https://doi.org/10.15292/acta.hydro.2018.06>.
- Sezen, C., Bezak, N., Bai, Y., Šraj, M., 2019. Hydrological modelling of karst catchment using lumped conceptual and data mining models. *J. Hydrol.* 576, 98–110. <https://doi.org/10.1016/j.jhydrol.2019.06.036>.
- Shaw, S.B., Riha, S.J., 2012. Examining individual recession events instead of a data cloud: using a modified interpretation of $dQ/dt-Q$ streamflow recession in glaciated watersheds to better inform models of low flow. *J. Hydrol.* 434–435, 46–54. <https://doi.org/10.1016/j.jhydrol.2012.02.034>.
- Staudinger, M., Stoelzle, M., Seeger, S., Seibert, J., Weiler, M., Stahl, K., 2017. Catchment water storage variation with elevation. *Hydrol. Process.* 31 (11), 2000–2015. <https://doi.org/10.1002/hyp.11158>.
- Teuling, A.J., Lehner, I., Kirchner, J.W., Seneviratne, S.I., 2010. Catchments as simple dynamical systems: experience from a Swiss prealpine catchment. *Water Resour. Res.* 46 (10), W10502. <https://doi.org/10.1029/2009WR008777>.
- White, W.B., 2002. Karst hydrology: recent developments and open questions. *Environ. Geol.* 65, 85–110. [https://doi.org/10.1016/S0013-7952\(01\)00116-8](https://doi.org/10.1016/S0013-7952(01)00116-8).
- White, W.B., 2007. A brief history of karst hydrogeology: contributions of the NSS. *J. Caves Karst Stud., National Speleol. Soc. Bull.* 69 (1), 13–26.
- Zhang, X., Huang, Z., Lei, Q., Yao, J., Gong, L., Sun, S., Li, Y., 2022. Connectivity, permeability and flow channelization in fractured karst reservoirs: a numerical investigation based on a two-dimensional discrete fracture-cave network model. *Adv. Water Resour.* 161, 104142 <https://doi.org/10.1016/j.advwatres.2022.104142>.